Journal of Hydrology 652 (2025) 132680

Contents lists available at ScienceDirect

Journal of Hydrology

journal homepage: www.elsevier.com/locate/jhydrol

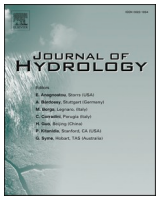

# Controls on runoff efficiency and its spatiotemporal variability in South Asian river basins

V.V. Sidhan [a], Manabendra Saharia [a,b,*]

[a] Department of Civil Engineering, Indian Institute of Technology Delhi, Hauz Khas, New Delhi 110016 India
[b] Yardi School of Artificial Intelligence, Indian Institute of Technology Delhi, Hauz Khas, New Delhi 110016 India

ARTICLE INFO

This manuscript was handled by A. Bardossy, Editor-in-Chief

*Keywords:*
Runoff Efficiency
ENSO
Indian Land Data Assimilation System (ILDAS)
Spatio-temporal analysis

ABSTRACT

Runoff efficiency (RE) represents the potential of a basin to generate runoff in response to precipitation and it varies based on climatology and physiography. It is a key metric that enables hydrologists to compare the hydrologic responses of basins across diverse climates and landscapes. In the large river basins of South Asia, RE plays a key role in floods and drought dynamics but has not been studied systematically. This study employs an integrated hydrologic-hydrodynamic modeling system, the Indian Land Data Assimilation System (ILDAS), to investigate the spatiotemporal variability of RE and their climatological and physiographic controls. The spatial variability of RE is mainly driven by mean precipitation and soil type. High RE is observed in the Central Indian basins, including Narmada, Brahmani, Godavari, and Mahanadi, due to high monsoon rainfall distribution and low permeability soils. However, large basins such as Brahmaputra, Ganga, and Subarnarekha exhibit low RE despite high monsoon rainfall, largely due to moderately permeable soil and significant baseflow contributions. Temporal variability in monthly RE influenced by event precipitation magnitude, antecedent soil moisture, and seasonal cycles, with the El Niño-Southern Oscillation (ENSO) exerting a notable influence at the interannual scale. La Niña events, particularly when coinciding with the monsoon season, enhance RE over the central eastern, central, and peninsular India, driven by ENSO's amplified impact on runoff relative to precipitation. Conversely, during the winter season in northern India, ENSO effects on precipitation don't translate into RE. Long-term trend analysis shows a rising trend in RE across several basins, during monsoon and pre-monsoon seasons, indicating an accelerated response of water cycle response linked to climate change. Notably, a positive trend in RE is observed in West Flowing Kachh-Sabarmati basins in the monsoon, pre-monsoon, and winter. Our findings enhance our understanding of the trends and drivers of RE and underscore the need for adaptive water management strategies in response to evolving patterns.

## 1. Introduction

The hydrological functioning of catchment systems in any given region has coevolved with the long-term climatology and physiography prevail in the region through reciprocal relationships functioning across multiple spatial and temporal scales. These long-term interactions and feedback induce variability in the hydrological process including runoff generation, and finally control the water availability for the human population. South Asia has a highly varying climatology due to unique geographical features like the Himalayan mountain ranges in the north and the Western (Eastern) Ghats in peninsular India, which provide a unique orographic effect that steers the atmospheric circulation and leads to diverse climatology (Gunnell, 1997). Hence, South Asia has hydrologically one of the most diverse catchment systems. Also, South Asia being home to one-sixth of the population around the globe is highly vulnerable to climate change, and the Intergovernmental Panel On Climate Change (IPCC) AR6 has reported that by mid 21st century, the transboundary basins such as Ganga and Indus could face a severe water crisis (Lee et al., 2023; Sivakumar & Stefanski, 2010). Similarly, owing to the climate regime shift in the late 1970 s, an intense change in the behavior of many hydroclimatic variables and associated extreme events is evidenced globally (Graham, 1994; Swanson & Tsonis, 2009). IPCC has reported that each of the last four decades has been successively warmer than any decade that preceded it since 1980 (Calvin et al., 2023). These variabilities in climate variables have brought an amplified effect on hydrological signatures and changes the water cycle dynamics

* Corresponding author at: Indian Institute of Technology Delhi, New Delhi 110016, India.
*E-mail address:* msaharia@iitd.ac.in (M. Saharia).

https://doi.org/10.1016/j.jhydrol.2025.132680
Received 4 June 2024; Received in revised form 29 December 2024; Accepted 1 January 2025
Available online 13 January 2025

and catchment responses (Hernandez et al., 2022). Runoff efficiency (RE; also referred to as runoff coefficient or runoff ratio) is the runoff generated per unit precipitation after satisfying intermediate demands such as evapotranspiration, deep percolation, and soil moisture storage. RE indicates the overall hydrological response of a catchment and its variability indirectly shows how the catchment is vulnerable to varying climate change impacts. Hence understanding the variability of RE in time and space across river basins in the region is important for adaptation planning, water supply design, flood management, etc. However, a comprehensive study on RE has been missing over the diverse river basins of South Asia.

RE is a key concept in engineering hydrology and an important diagnostic variable for basin performance, particularly useful for a comparison study of a diverse catchment using a single indicator (Merz & Blöschl, 2009). Higher rainfall generally results in higher runoff and hence the idea of dividing the runoff by precipitation is to nullify the impact of rainfall effect on runoff generation. Thereby, it aids in studying the basin's potential to generate runoff. RE varies across different catchments and long-term controls such as climate or basin landscape characteristics that do not vary at a short time scale contribute to the spatial variability of the mean runoff coefficients (Norbiato et al., 2009). Merz & Blöschl (2009) examined the runoff coefficient's controls over Australian catchments and identified that the mean precipitation and antecedent soil moisture (AMC) play a major role. Similarly, Norbiato et al., (2009) also showed that the mean runoff coefficient of a basin increases with annual mean rainfall, and the geological effect is significant for those catchments with annual mean rainfall less than 1200 mm. McCabe & Wolock (2016) investigated the variation of RE over the conterminous United States and observed a high RE associated with high precipitation region. Woodhouse & Pederson (2018) reported that temperature has a significant role in the RE over the upper Colorado river streamflow. Most of the studies have identified climatology as the dominant control of spatial variability runoff coefficient while a few studies have also shown the role of basin characteristics especially in hilly and smaller catchments (Abdulkareem et al., 2018; Akhil et al., 2022; Mangan et al., 2019). Although climate and basin characteristics are two different factors, at a larger time scale, they have a certain level of dependency, and they are co-evolved by mutual interaction. A basin's current climate and landscape are the product of long-term reciprocal interactions, mediated by material and energy flows in response to slow geological processes and quicker climate dynamics (Sivapalan, 2005).

RE of a basin also varies with time, especially showing seasonal cycles which are mainly controlled by the AMC that fluctuate with seasonal precipitation (Merz & Blöschl, 2009). Similarly, RE can also influenced by longer time-scale (inter-annual and multi-decadal) fluctuations due to natural climate cycles such as El Niño-Southern Oscillation (ENSO), Pacific Decadal Oscillation (PDO), Equatorial Indian Ocean Oscillation (EQUINOO), etc. El Niño-Southern Oscillation (ENSO) is a Sea Surface Temperature (SST) anomaly pattern in tropical Pacific Ocean but have significant effect on the climate around the world through ocean-atmospheric interaction (Chang et al., 2001; McPhaden et al., 2006; Sarachik and Cane, 2010; Singh et al., 2015; Rodríguez-Fonseca et al., 2016; Chen et al., 2018; Tamaddun et al., 2019; Park et al., 2020). ENSO has shown a significant impact on the South Asian climate and it is well established that a higher monsoon precipitation is received during the La Niña phase over different parts of India (Hrudya et al., 2021; L. Krishnamurthy & Krishnamurthy, 2016; V. Krishnamurthy & Goswami, 2000). In addition to its impact on temperature and precipitation, climate oscillations also affect the hydrological signatures, especially runoff. Hussain et al. (2022) show that runoff variability in the source region of the Indus River basin is significantly influenced by climate indices like the North Atlantic Oscillation (NAO) and Arctic oscillation (AO). Also, Hernandez et al. (2022) showed that in the hydrological regimes of Chile, ENSO has an amplified effect on the streamflow compared to the precipitation. Hence, ENSO influence on the precipitation might not directly translate to surface hydrological responses, rather it can be either amplified or diminished, due to its effects on other climate drivers. Soden (2000) has studied the influence of ENSO on the hydrological cycle and observed that a variation in the precipitation intensity, temperature, and water vapor mass in the tropical atmosphere results in a more intense hydrologic cycle. Hence the influence of these climate signals is complex, and its effect on precipitation and temperature might not directly be translated to the RE.

In addition to the cyclic variations, climate change due to global warming and other anthropogenic interventions can lead to long-term trends in the mean RE of a basin. One of the consequences of global warming is the water cycle intensification which increases the evapotranspiration and changes the precipitation pattern of a basin (Allan et al., 2020; Durack et al., 2012; Huntington, 2006). In some regions, atmospheric warming increases the precipitation along with evapotranspiration and makes no changes to runoff generation. On the contrary, the precipitation decreases in some areas further aggravate the consequences of increased evapotranspiration, and the net effect reduces the runoff (Zhang et al., 2001). In a study, Nowak et al. (2012) observed that a one degree warming is expected to decrease RE by 2 % in the Upper Colorado River basin. In another study of the variability of RE in the Upper Mississippi River Basin (UMRB), Frans et al., (2013) found that growing regional precipitation is the cause of the positive trend in runoff. In addition to climate change due to global warming, land use land cover (LULC) changes by human activities also cause long-term trends in runoff generation (Astuti et al., 2019; Frans et al., 2013). However, the effect of LULC on RE is more localized and is related to the spatial scale (Norbiato et al., 2009). Generally for larger-scale studies, LULC has a lesser role on RE while their effect is significant in smaller-scale and hillslopes as illustrated in several plot studies (Astuti et al., 2019; Kirnbauer et al., 2005). Thus, climate change plays a significant role in the temporal variability of RE, and RE is the final response of a basin whose variability can further show the basin's sensitivity to climate change.

The intricate climatic conditions and diverse landscapes of South Asian basins result in complex relations between rainfall and runoff. RE is a key metric that enables hydrologists to compare basins with diverse climates and landscapes, providing insights into their hydrological behavior and water resource management. In addition, analyzing the RE of different catchments over a longer period is crucial for understanding changes in the water cycle dynamics, particularly in response to climate change and global warming. While the interannual variability in precipitation and temperature across South Asia due to ENSO is well-documented, its impact on RE remains unexplored. A comprehensive analysis of the spatio-temporal variability of RE and their controls over South Asian basins is lacking except in a few regional studies that consider RE of specific events (Sharma et al., 2019; Z. Zhang et al., 2014). The requirement of continuous hydroclimate data such as baseflow, soil moisture, and evapotranspiration, in addition to surface runoff data over the South Asian basins, is one of the main constraints for conducting such a study. The Indian Land Data Assimilation System (ILDAS) is a multi-model hydrologic-hydrodynamic modeling system set up over South Asia that can estimate land surface states and fluxes, including runoff (Magotra et al., 2024a).

This study performs a comprehensive analysis of the spatiotemporal variability and trend in RE for the South Asian basins and investigates the following science questions:

1) What are the factors that affect the spatial and temporal variability of RE?
2) How does the teleconnection of ENSO on precipitation over South Asia translate to surface runoff and RE?
3) Are there any trends in RE over South Asia and what are its causes?

## 2. Materials and Methods

### 2.1. Study area

The study focuses on the major river basins within India and three transboundary basins that share boundaries with the neighboring countries such as *Pakistan, Bangladesh, Bhutan, China, Nepal, Afghanistan, and Myanmar*, spanning 64.5° E – 98° E and 5.5° N – 37.5° N (Fig. 1). It encompasses 15 major river basins within the Indian subcontinent and three transboundary basins: the Indus, Ganga, and Brahmaputra. West Flowing Kachh-Sabarmati is denoted as WFKS, and East Flowing rivers Mahanadi-Pennar and East Flowing Pennar-Kanyakumari are together represented in the map as EEMP, and EFPK respectively.

### 2.2. Hydrological model

This study utilizes the Indian Land Data Assimilation System (ILDAS), which is a coupled hydrologic-hydrodynamic modeling system setup over South Asia and provides reliable estimates of land surface conditions and fluxes, including water balance components (Magotra et al., 2024). NASA Land Information System Framework (LISF) serves as the foundation for the ILDAS. LISF is an open-source tool that facilitates a multi-model, multi-forcing approach to land surface modeling (Kumar et al., 2006). For this study, we use the NoahMP 4.0.1 model (Niu et al., 2011), which is the advanced version of the older Noah model (Ek et al., 2003) with multi-parameterization functionality that takes into account more recent developments in land surface physics such as a tiling scheme in the grid, which can differentiate between vegetation and bare soil, several layers of snowpack as opposed to a single bulk layer of snowpack. The LSM generates terrestrial water balance components such as evapotranspiration, surface runoff, soil moisture, baseflow, etc. The model simulations were configured to run at a higher spatial scale of 0.10° resolution from 1981 to 2021 and the output data was generated at a daily temporal scale. The detailed specification of the different components of ILDAS is given in Table 1. In

**Table 1**
ILDAS components and their specifications.

| ILDAS component | Specification |
|---|---|
| Land Surface Model | Noah-MP 4.0.1 |
| Spatial Extent | 64°E-98°E, 5.5°N-37.5°N |
| Spatial Resolution | 0.1° |
| Temporal Resolution | 1 Day |
| Time Period | 1981–2021 |
| Forcing | IMD (for precipitation) and MERRA2 (for rest of the forcing variables) |
| Forcing Variables | Precipitation, surface pressure, near-surface air temperature, eastward and northward wind velocity, incident longwave, near-surface specific humidity, and shortwave radiation |
| Soils Definition | (NCAR) STATSGO + FAO blended soil texture map |
| Vegetation Definition | MODIS-IGBP (NCEP-modified), Monfreda et al. (2008) |
| Output format | NetCDF |

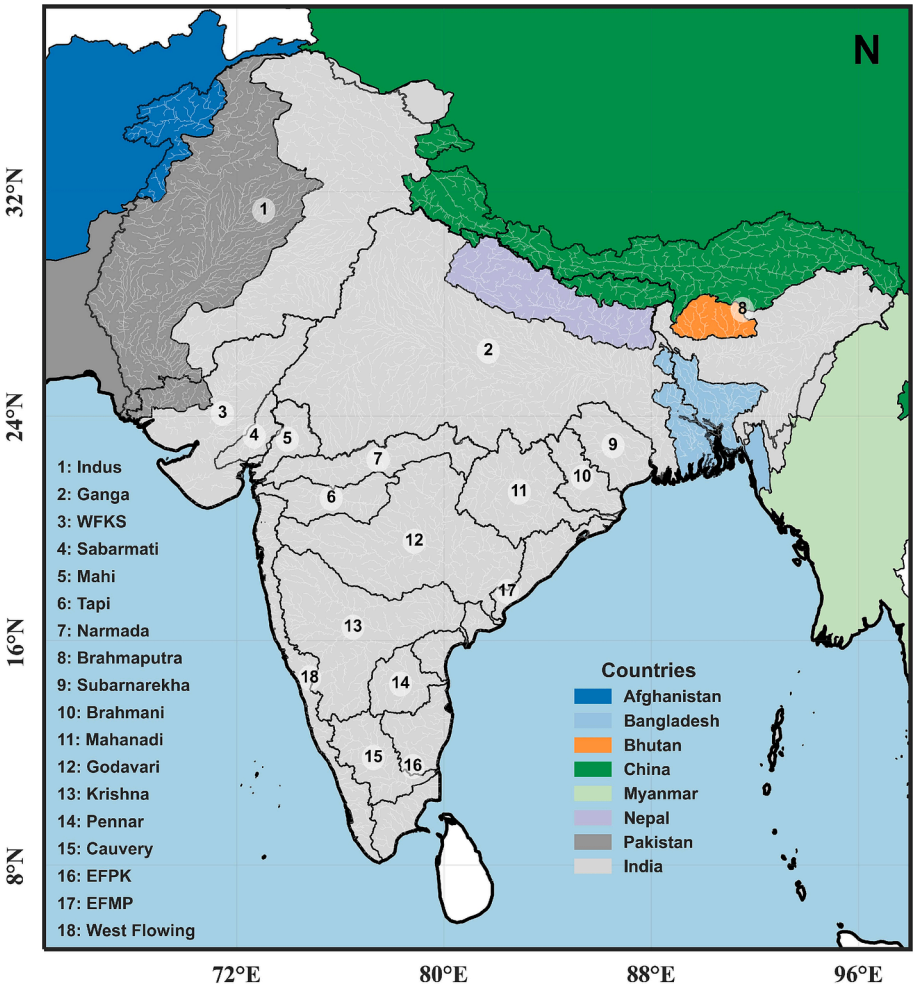


**Fig. 1.** Map of the study area showing various river basins and their country boundaries.

this study, we have utilized the surface runoff, soil moisture, and baseflow outputs from the ILDAS model to study the spatial–temporal variation of runoff efficiency and its controls. The overall methodology flowchart of the study is shown in Fig. 2.

We used the gridded precipitation during 1981–2021 at 0.25° spatial resolution from the Indian Meteorological Department (IMD) as the meteorological forcings of ILDAS. The dataset is created using 6955 gauge stations which include IMD observatory stations, hydrometeorological observatories, and agrometeorological observatories (Pai et al., 2015). The data outside the geographical boundaries of India are supplemented with the MERRA-2 (Modern-Era Retrospective Analysis for Research and Applications, Version 2) as South Asia extends beyond the IMD precipitation domain. Studies such as Magotra et al. (2024b) have found that overall IMD precipitation outperforms other precipitation (MERRA-2, ERA-5, CHIRPS) for simulating runoff within India by ILDAS. The Modern-Era Retrospective Analysis for Research and Applications, Version 2 (MERRA-2; Gelaro et al., 2017) is an updated version of its predecessor, MERRA, by utilizing the current progress at NASA's Global Modeling and Assimilation Office (GMAO). The new assimilation schemes for NASA ozone observations, microwave observations, hyperspectral radiance, and many more datatypes are included in the MERRA-2.

### 2.3. Precipitation, Runoff, soil moisture and baseflow

The study uses the IMD precipitation data along with the surface runoff, soil moisture, and baseflow output from ILDAS. The data are available from 1981 to 2021 at a spatial resolution of 0.1 x 0.1 at a daily timestep and are aggregated to a monthly scale. Runoff efficiency is calculated for the whole domain using the following equation:

$$RunoffEfficiency = \frac{Monthlysurfacerunoff}{Monthlyprecipitation} \quad (1)$$

The soil moisture and baseflow data were utilized to study the controls influencing the spatio-temporal variability of RE. The study uses the standard definition of seasons for South Asia: pre-monsoon (MAM, March-May), monsoon (JJAS, June-September), post-monsoon (OND, October-November), and winter (DJF, December-February).

### 2.4. Soil group and land use land cover (LULC) data preparation

In this study, we have used soil properties such as clay, sand, and silt content to study the influence of soil on the spatial variability of RE. The soil texture classes are derived using the soil properties as suggested by the Natural Resources Conservation Service Soils (NRCS) of the United States Department of Agriculture (USDA). The NRCS-USDA has developed a Soil Texture Calculator Triangle, which categorizes soil into different texture classes based on the proportion of sand, silt, and clay content (Table 2). For the hydrological applications, the soil texture classes are further reclassified into four hydrological soil groups (HSG) based on their runoff potential (Ross et al., 2018). Groups A, B, C, and D exhibit low, moderately low, moderately high, and high runoff potential, respectively (Table 2). The datasets are downloaded from SoilGrids which is a platform where the soil profile datasets are processed using machine learning techniques to produce digital soil maps across the globe.

The LULC is another factor that influences RE. The LULC map of 2020 from the Environmental Systems Research Institute (ESRI) is utilized in this study. The ESRI nine classification map is reclassified into 6

**Table 2**
Ranges of contents of sand, silt, and clay for texture classification (NRCS-USDA).

| Texture Class | Sand (%) | Silt (%) | Clay (%) | HSG |
|---|---|---|---|---|
| Sand | 85–100 | 0–15 | 0–10 | A |
| Sandy loam | 43–85 | 0–50 | 0–20 | B |
| Loamy sand | 70–90 | 0–30 | 0–15 | B |
| Loam | 23–52 | 28–50 | 7–27 | C |
| Silt loam | 0–50 | 50–88 | 0–27 | C |
| Sandy Clay Loam | 45–80 | 0–28 | 20–35 | C |
| Clay Loam | 20–45 | 15–53 | 27–40 | C |
| Sandy Clay | 45–60 | 0–20 | 35–55 | D |
| Silty Clay loam | 0–20 | 40–73 | 27–40 | C |
| Clay | 0–45 | 0–40 | 40–100 | D |
| Silty Clay | 0–20 | 40–60 | 40–60 | D |
| Silt | 0–20 | 80–100 | 0–12 | C |

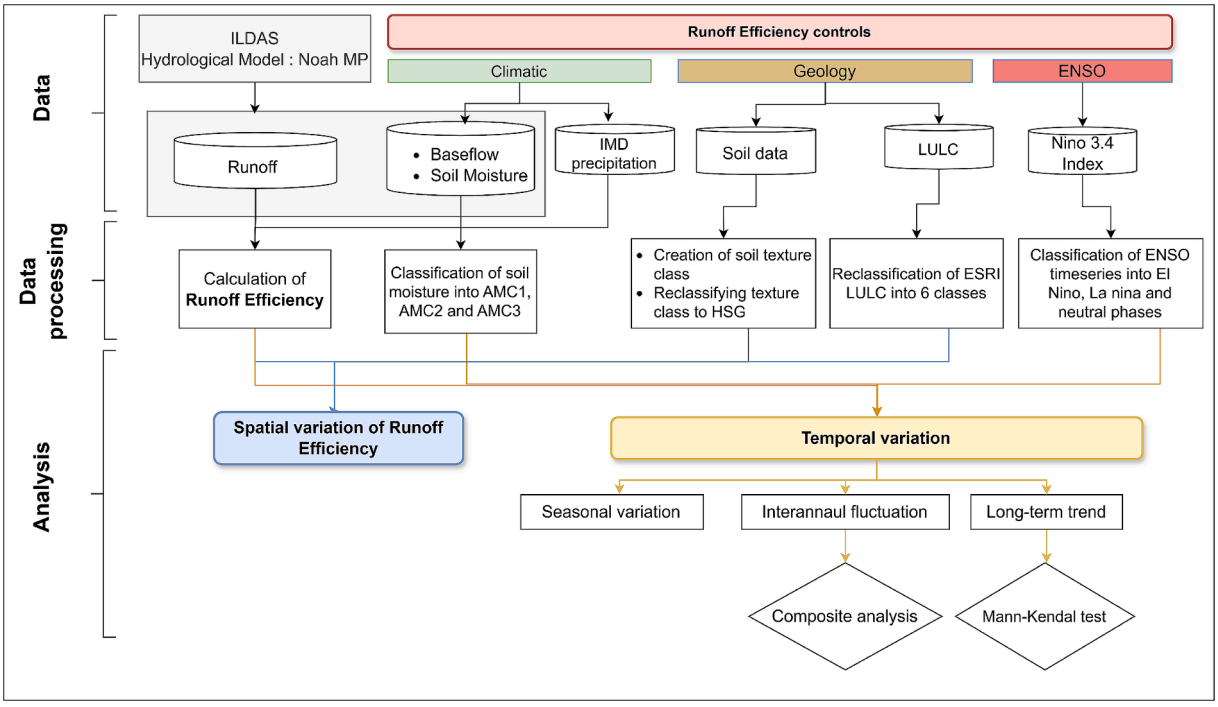


**Fig. 2.** The overall methodology flowchart of the study.

classes comprising Built-up area, agricultural land, Evergreen-Broadleaf forest, Shrubland/Wasteland, Water Bodies, and Ice-Glaciers (Fig. 3c). Further, we have computed the curve number developed by Soil Conservation Service (SCS) which combines the effect of LULC maps and hydrological soil groups to give a single numerical value which is proportional to runoff potential of a region (Kumar et al., 2010) (Table S1).

### 2.5. Teleconnection and trend analysis

In this study, we investigated the teleconnection between RE and ENSO. The Niño 3.4 is used as the monthly ENSO index, and it represents the average SST anomaly between 5°S–5°N and 170°W–120°W. El Niño/ La Niña occurs when the Niño 3.4 index is greater/ lesser than + 0.4/-0.4 for six consecutive months (Trenberth, 1997; Trenberth & Stepaniak, 2001). Thus, the months in the period from 1981 to 2021 are classified into El Niño, Neutral, and La Niña phases according to the Nino 3.4 index.

For the teleconnection analysis, we used the technique of composite and grouping (Hernandez et al., 2022). Firstly, we calculated the standardized monthly anomaly of precipitation, surface runoff, and RE time series for consistent comparison between variables ($Z_t$). Then, the ENSO-composites of this standardized variable are computed as the average of these variables associated with specific ENSO phases, El Niño and La Niña. Then an additional composite is calculated as the difference between the La Niña and El Niño composites which gives the amplitude of the ENSO-related shift.

$$\text{Composite}_{\text{La Niña}}\ ofz := \text{mean}\,(z_t)_{t\in \text{La Niña}} \tag{2}$$

$$\text{Composite}_{\text{El Niño}}\ ofz := \text{mean}\,(z_t)_{t\in \text{El Niño}} \tag{3}$$

$$\text{Composite}_{\text{La Niña - El Niño}}\ ofz := \text{mean}\,(z_t)_{t\in \text{La Niña}} - \text{mean}\,(z_t)_{t\in \text{El Niño}} \tag{4}$$

z ∈ Rainfall/ Runoff/ RE and $z_t$ represents the value of variable z at

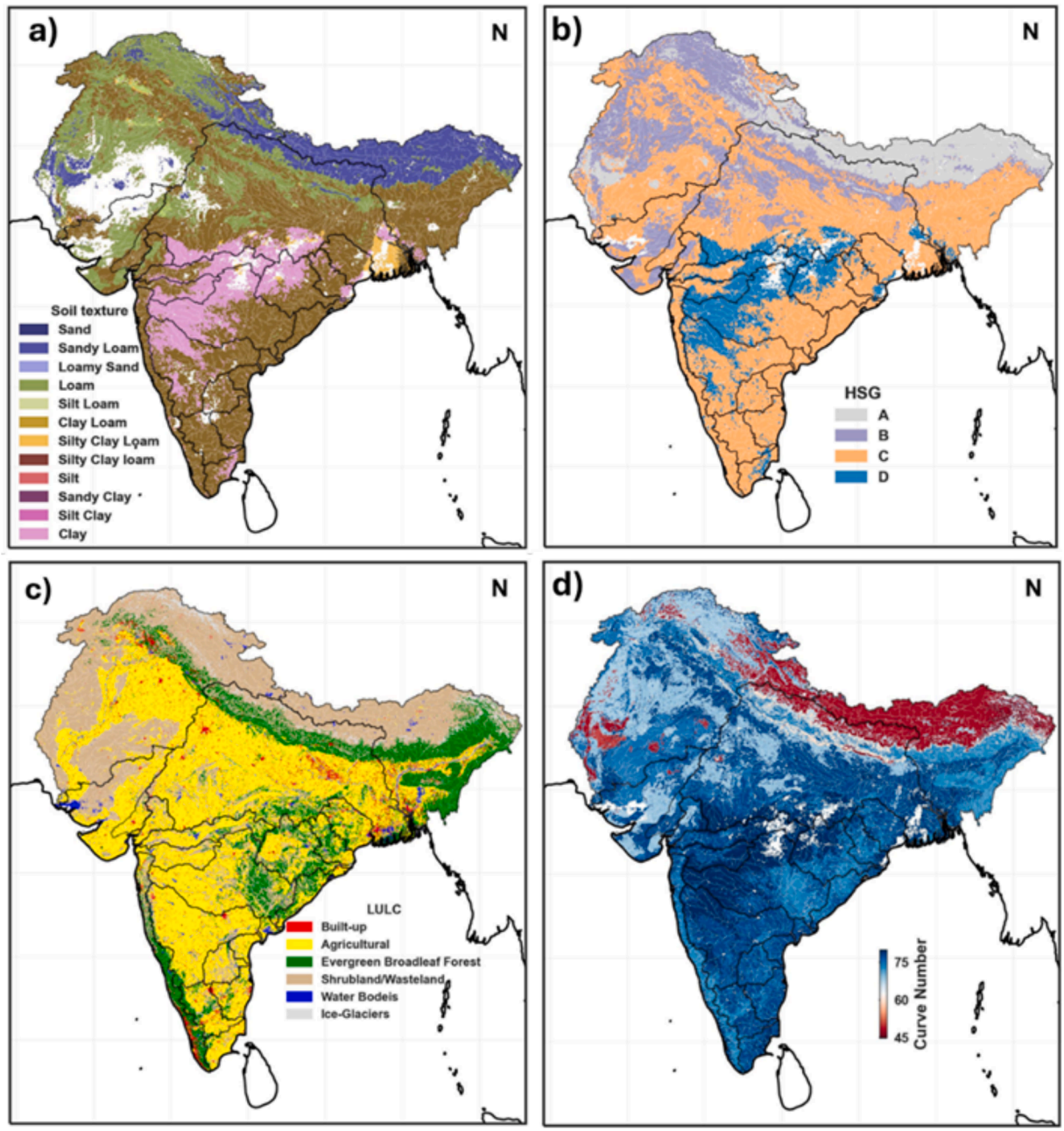


**Fig. 3.** Map showing (a) soil texture classification, (b) hydrological soil groups, (c) land use land cover types, and (d) curve number in South Asian river basins.

time t.

This study investigated the trend in the timeseries of precipitation, runoff, and RE using the Mann-Kandall (MK) test (Mann, 1945). Mann-Kandall is a non-parametric test, mainly used to statistically detect trends in meteorological and hydrological timeseries (Burn et al., 2004; Chandole et al., 2019; Jain et al., 2013; Joshi et al., 2016; Kaur et al., 2017; Meshram et al., 2017). Since its statistics are based on positive and negative signs, one of the advantages is its ability to handle outliers in the form of extreme values in hydrological time series (Helsel & Hirsch, 1992). The MK test evaluates the significance of trend using the test statistics at a 5 % significance level with the null hypothesis H0 stating that there is no significant trend in the time series. The Mann–Kendall test begins with the calculation of S statistics:

$$S = \sum_{i=1}^{n-1} \sum_{j=i+1}^{n} \mathrm{sgn}(k_i - k_j) \tag{5}$$

Where $k_i$ and $k_j$ are the data values in $i^{th}$ and $j^{th}$ time of observation.

$$\mathrm{sgn}(k) = \begin{cases} +1 \text{ if } (k_i - k_j) > 1 \\ 0 \text{ if } (k_i - k_j) = 0 \\ -1 \text{ if } (k_i - k_j) < 1 \end{cases} \tag{6}$$

The Z statistic is computed:

$$Z = \begin{cases} \dfrac{S-1}{\sqrt{\mathrm{Var}(S)}} & \text{if } S > 0 \\ 0 & \text{if } S = 0 \\ \dfrac{S+1}{\sqrt{\mathrm{Var}(S)}} & \text{if } S < 0 \end{cases} \tag{7}$$

$$(S) = \frac{n(n-1)(2n+5) - \sum_{i=1}^{t} t_i(t_i-1)(2t_i+5)}{18} \tag{8}$$

where, n is the number of data points, and ti is the number of ties for the ith value.

One of the issues with MK test is that it shows a significant trend in the absence of trend when the time series exhibit significant autocorrelation and leads to misleading interpretations (Burn et al., 2004). Hence, we have considered the standardized monthly anomaly of the time series which eliminates the autocorrelation due to seasonality in the time series.

## 3. Results and discussions

Runoff Efficiency (RE) represents a basin's ability to generate runoff from precipitation, which varies spatially and temporally. Fig. 4 shows the spatial variation of climatological mean and variance of RE from 1981 to 2021 for different seasons. The mean monthly RE over South Asian river basins goes up to 0.35 in the wettest months. The mean RE is higher in the Central Indian basins and it is maximum in the monsoon season. Fig. 5a shows the boxplot of regional mean RE in different seasons over the 18 basins in South Asia. The monsoon core basins such as Narmada, Brahmani, Godavari, West flowing, and Tapi exhibit high mean RE. Narmada basin shows the highest RE among all with a mean RE value of 0.25 in the monsoon season. Similarly, Brahmani basins have relatively higher RE throughout the year. In EFMP and EFPK basins, a higher RE is observed in post-monsoon and winter respectively. Brahmaputra, Ganga, Subarnarekha, Krishna, and Cauvery exhibit relatively low basin performance.

Similarly, the variance of RE has been investigated using the coefficient of variation (CV). CV is calculated by the standard deviation of RE divided by the mean rainfall. It shows the least in the region of high mean RE, whereas the largest in the region of low mean RE (Fig. 4 e-f). Similar results have been reported by Merz et al. (2006) and they concluded that the RE variability between events is low in catchments with larger mean RE. However, when we use standard deviation (Sdev) instead of CV, the observation is reversed showing a higher Sdev wherever mean RE is higher (see supplementary Fig. S1). Two issues with comparing the variance of climate variables across different regions are the skewness exhibited by data and the varying range of data at different regions. This results in regions with higher means artificially showing higher Sdev. Although using the CV (Dividing Sdev by the mean) can solve the former, but the issue is further exacerbated by overweighting regions with higher mean due to skewness. Ultimately, the region with a high mean shows a lower CV value and it can be clearly seen in Fig. 4. Thus, using Sdev/ CV to compare the variance of

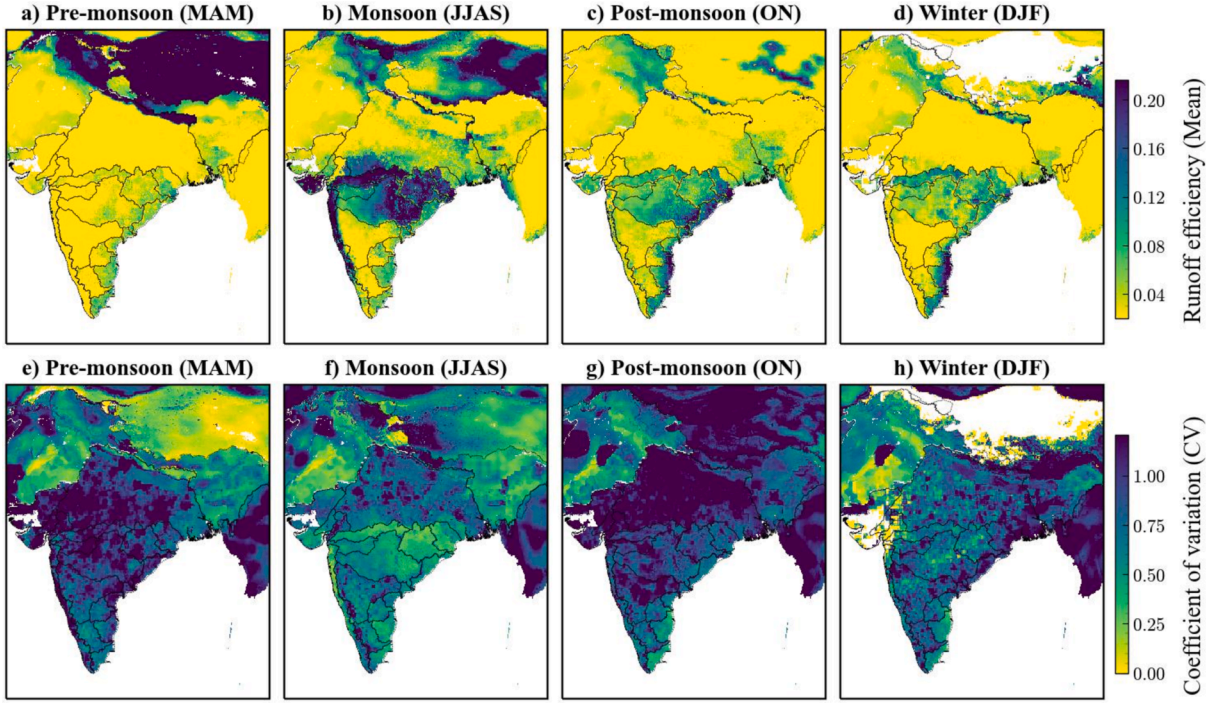


**Fig. 4.** Seasonal mean and variance of RE for pre-monsoon, monsoon, post-monsoon, and winter seasons.

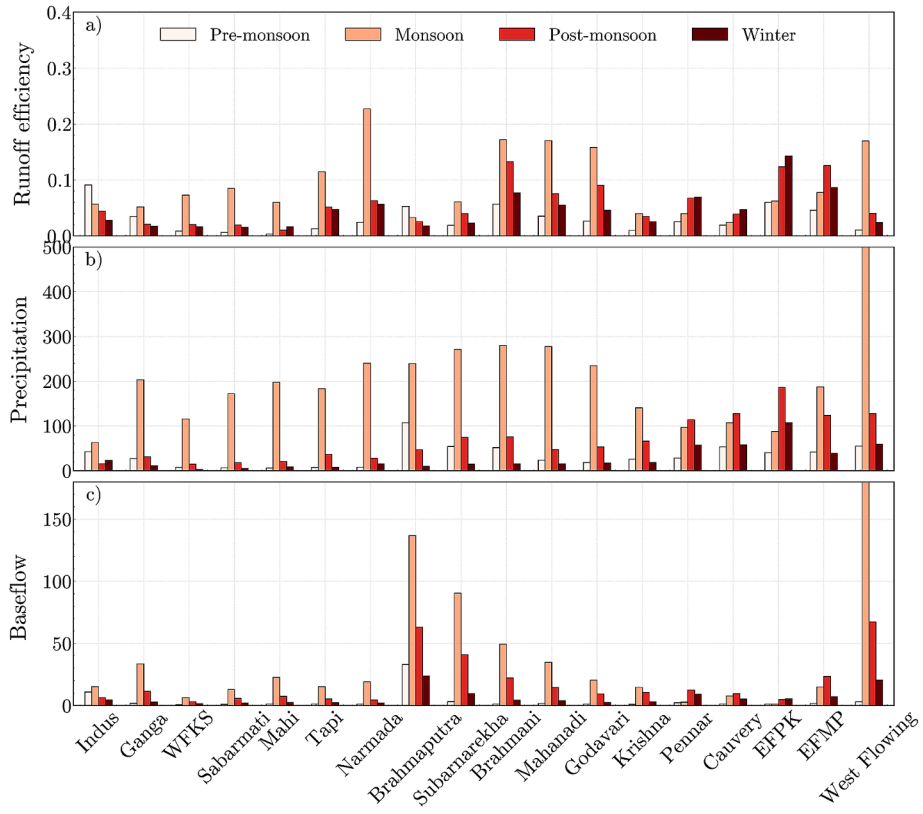


**Fig. 5.** Seasonal mean of RE, precipitation, and baseflow over South Asian river basins.

hydrometeorological variables across regions results in misleading assessment.

A close comparison between the mean RE bar plot (Fig. 5a) and the mean precipitation bar plot (Fig. 5b) reveals that mean RE is higher wherever mean precipitation is high (see Fig. S2 for all grids). A high correlation of 0.6 is obtained between mean RE and mean precipitation over the study area (see supplementary Fig. S3). Similar results are reported by McCabe & Wolock (2016), who found that the RE over the conterminous US is high in the wettest part of the country. The soil in the area with higher mean precipitation is consistently moist and has more runoff potential (Merz & Blöschl, 2009; Norbiato et al., 2009). Thus, the mean RE is strongly influenced by mean precipitation in a region, but the underlying factor is the soil moisture content. In addition, from Fig. 3a, it can be observed that the soil in these Central Indian basins is characterized by high clay content and belongs to the hydrological soil group D (Fig. 3b). This soil group has inherently high runoff potential owing to low permeability of clayey soils, resulting in slower infiltration rates. Hence, along with high mean precipitation, the less permeable soil type contributes to high RE at these Central Indian basins. The fact that both mean precipitation and soil type in these Central Indian basins act in the same direction is not merely coincidental. At a longer timescale, mean annual precipitation influences the soil physiography by controlling the soil formation and erosion process. The soils in the Central Indian basins are primarily Luvisols and Vertisols, which are mainly developed as a result of high seasonal rainfall, leading to the formation of clay-rich soils with low permeability (Ahmad, 1996, 1996). Hence, climate and geology have a certain level of dependency, as highlighted by Norbiato et al. (2009), that the regions with high precipitation are often characterized by low-permeability soils.

However, certain basins exhibit deviations from this general observation of higher RE in basins where there is high mean rainfall. For instance, Brahmaputra, Subernareksha, and Ganga have low RE despite receiving higher monsoon precipitation (Fig. 5b). Similarly, RE is relatively lower in the West Flowing basins, which receive almost double the monsoon precipitation as Narmada (Fig. 5a). This is due to the dominant effect of basin landscape characteristics over the climatology. From the soil map (Fig. 3b), it can be observed that these basins belong to either soil group C or B, which have moderate runoff potential. In addition, the West flowing river basins have forest land cover, which again reduces runoff potential. However, overall the LULC has less effect on the spatial variability of RE over the study area (see supplementary Fig. S3). In West flowing river basin, climatology and soil type, act in opposite directions and result in a moderate RE, unlike the case of Central Indian basins. Also, we investigated the baseflow component (Fig. 5c), which arises from soil infiltration, and serves as an indirect representation of the subsurface soil attributes of the basin. The result shows that the West flowing, Ganga, Brahmaputra, and Subernarekha basins have more baseflow contribution pertaining to the moderately/ high permeable soil type (Fig. 5c). Ultimately, RE is influenced by the complex interplay of climatology and soil type, with the dominance of either factor varying by region. The overall hydrological performance of a basin is a trade-off between its climatological and landscape characteristics. For those basins belonging to arid/semi-arid climates where precipitation is a limiting factor, RE predominantly depends on basin physiography. While in humid regions where rainfall is abundant, the RE variability is more influenced by climatology.

To further investigate the effect of monthly precipitation magnitude, AMC condition, and seasonal cycle on RE, a monthly rainfall-RE scatter plot has been studied (Fig. 6). The observations in different seasons are represented with colors, and AMC conditions are represented with shapes. We have classified the soil moisture condition into three different classes, AMC1 (0–30 percentile), AMC2 (30–60 percentile), and AMC3 (above 60 percentile). It is observed that the rainfall-RE plot follows a non-linear relation as the curve steeps upwards for lower precipitation and then becomes less steep. Thus, precipitation magnitude has a clear role in monthly RE. A steeper curve is observed in the Central Indian basins, showing a strong response to precipitation magnitude, and it is due to the presence of clayey soil. The influence of

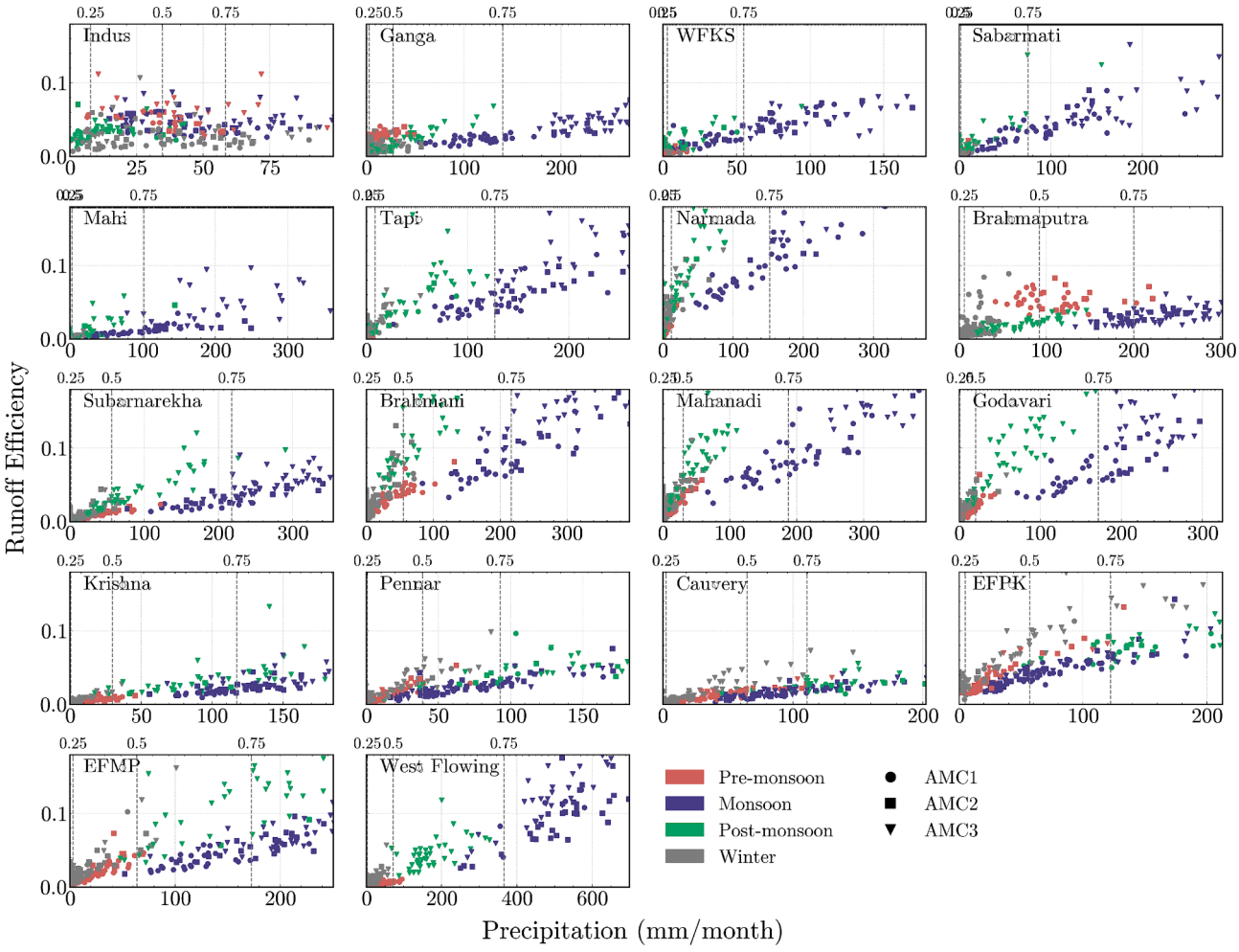


**Fig. 6.** Scatter plot between precipitation and RE for different basins over the study area. The colours represent different seasons and the shapes represent AMC conditions.

AMC is clear as we can observe that, for the events of the same precipitation magnitude, the RE associated with AMC3 (triangle) shows high values (Fig. 6). For instance, in the river basins such as Brahmani, Godavari, and Subarnarekha River basin, even for a lesser precipitation magnitude (50–150 mm/month), RE is higher whenever the soil moisture condition is in AMC3 (green triangle) (Fig. 6). This shows the relatively dominant impact of soil moisture conditions over precipitation magnitude and it is in agreement with Merz & Blöschl (2009). Hence, RE is controlled by the relative effect of monthly precipitation magnitude and AMC conditions, which can vary based on basin geology. Apart from these two factors, the seasonal distribution of rainfall also plays a major role in the temporal variability of RE (see Fig. 5a and Fig. 6). It is observed that basins that receive higher monsoon rainfall show a higher RE in the post-monsoon season (Fig. 5). Similarly, in basins such as Pennar, Cauvery, and EEPK where the post-monsoon rainfall is dominant, winter RE is relatively higher (Fig. 5). Basically, season and AMC condition are highly dependent as we can observe that most of the AMC3 (triangle) condition are associated with post-monsoon (green) in all the basins irrespective of rainfall magnitude (Fig. 6). These can be due to soil already being recharged during the summer monsoon and hence a higher portion of the rainfall is being converted to runoff in post-monsoon. For instance, in the Brahmani basin, despite receiving lesser precipitation magnitude in post-monsoon, a relatively higher RE is observed as the soil is in the AMC3 condition (Fig. 6). Thus, temporal variability of monthly RE is mainly controlled by the relative effect of precipitation magnitude, AMC condition, and season, with these factors exhibiting a certain degree of interdependence.

### 3.1. *ENSO influences on the climate variables and runoff efficiency*

Fig. 7 shows the composite anomalies (El Niño minus La Niña averages) of precipitation, runoff, and RE during different seasons. The result shows that there is a statistically significant influence of ENSO on the study domain. It has been noticed that there is significant seasonal variation in the teleconnection of ENSO. During the monsoon season, a positive composite anomaly is observed in Central East, Central, and Peninsular India, which shows excess rainfall during La Niña. It is consistent with the general understanding that La Niña brings above-normal precipitation in India during the monsoon (Gadgil et al., 2007; Hrudya et al., 2021; L. Krishnamurthy & Krishnamurthy, 2016). The bar plot showing the regional composite average of El Niña and La Niña phases during the monsoon season is also shown in Fig. 8. It can be observed that the precipitation is significantly higher in the La Niña phase for the basins such as Godavari, Brahmani, Mahanadi, Subarnarekha, Pennar, and Ganga. RE was also observed to increase during La Niña. Also, the influence of ENSO on RE follows the same spatial pattern as runoff and it is slightly amplified in central India and suppressed over northern India (Fig. 7). An amplified response of runoff on ENSO compared to the precipitation could be the reason for the modulation of RE. The numbers in the barplot (Fig. 8) show the amplification ratio, indicating the strength of ENSO impact, and it is the ratio between the El Niño and La Niña composites. Over Central Eastern India, the

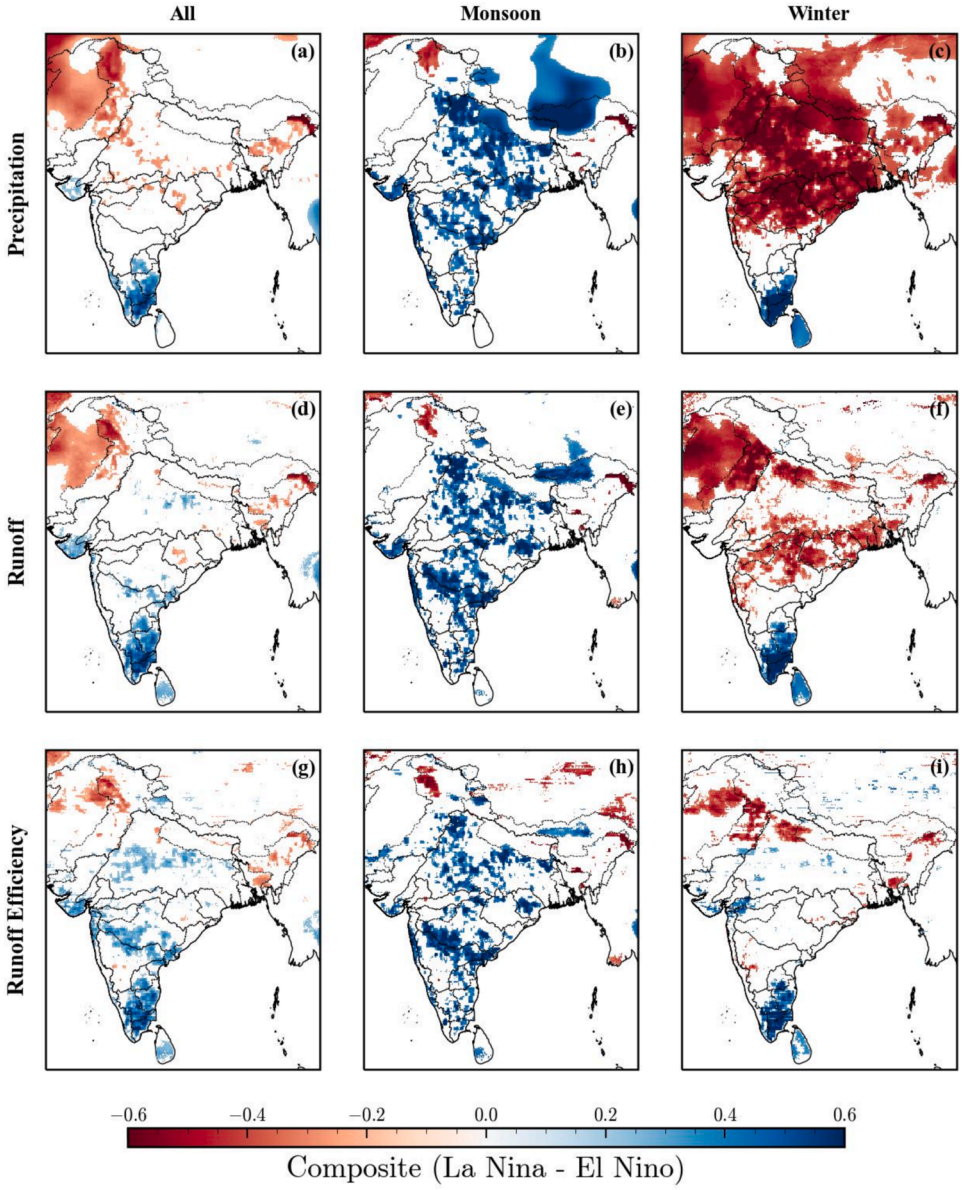


**Fig. 7.** Map of the composite analysis (El Niño- La Niña) of Precipitation, runoff, and RE for different seasons. Only regions passing the Mann-Whitney test at a 5% level significance level are shown.

amplification ratio of runoff is found to be greater than that of precipitation, indicating that the impact of ENSO on rainfall is amplified over runoff. For instance, in the Godavari river basins, the ratio is 1.31 for precipitation, and it is increased to 1.83 for runoff, and the net increase in RE is 1.41. During the winter, the effect of ENSO on the precipitation is reversed and it is shifted towards North India and some parts of Southern India. In Northern India, a negative composite anomaly prevails, indicating that rainfall during El Niño phases is higher. Rainfall is brought by the Western disturbance during this period and hence lower/ higher rainfall during La Niña/ El Niño phases is the result of ENSO interaction with Western disturbances (Dimri, 2013; Krishnan et al., 2009).

The result of the regional composite analysis during the winter season is given in the supplementary fig. S4. Although ENSO has a significant effect on North Indian rainfall in winter, it has not been translated to runoff and RE during the winter (See supplementary fig. S4). Unlike North India, a positive composite rainfall anomaly is observed in Southern Indian basins (Cauvery and EFPK) during winter season which translates to runoff and RE. The Northeast monsoon brings rainfall to these basins during the post-monsoon period (Rajeevan et al., 2012). Overall, it could be said that La Niña always enhances the monsoon rainfall (Southwest monsoon and Northeast monsoon) and depreciates the Western depression rainfall that results in positive/ negative composite anomaly in the monsoon/ Western disturbance affected basins.

### 3.2. *Trend analysis of runoff efficiency*

The variables precipitation, runoff, and RE are subjected to standardization, and long-term trend analysis for the period 1980–2021 is carried out using Mann-Kendall test (Fig. 9). Trend analysis of each season was investigated separately as previous studies has clearly reported the varying trends across seasons within the same region (Guhathakurta & Rajeevan, 2008). In the Monsoon season, a positive trend in RE, runoff, and rainfall is recorded in the WFKS. The increase in monsoon precipitation in the Kutch, Saurashtra, and Marwar basins are reported in the previous studies (Agnihotri et al., 2017, 2018; Krishnan et al., 2020; Yadav et al., 2021). The trend in RE shows that the runoff production/basin activity is increasing with time, and more runoff is

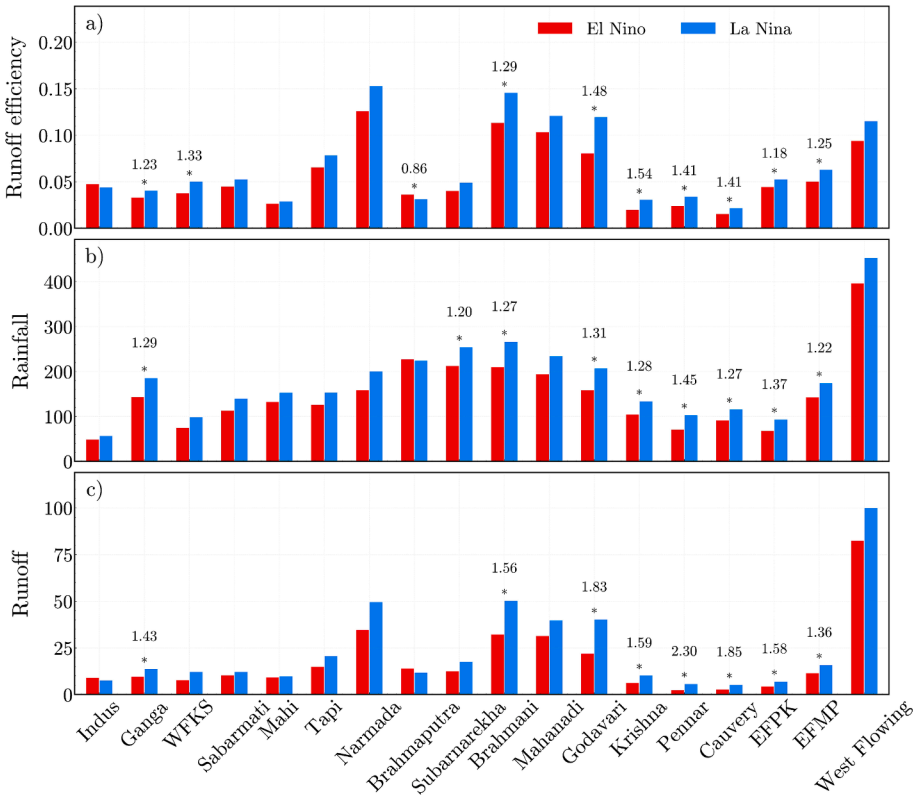


**Fig. 8.** Composite analysis (El Niño-La Niña) result of the regional average of precipitation, runoff, and RE for the Monsoon season. '*' shows the regions showing statistically significant differences between El Niño and La Niña events. The number represents the ratio between El Niño and La Niña composites.

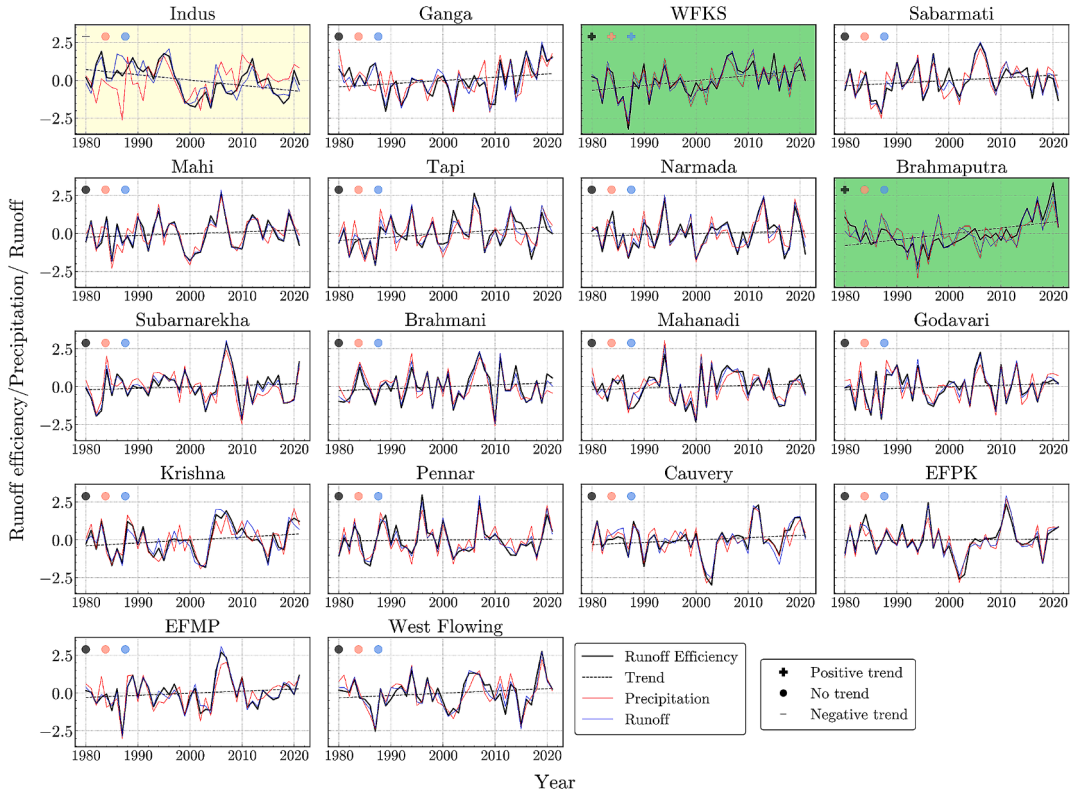


**Fig. 9.** Monthly time series of RE, precipitation, and runoff in the monsoon season during 1980–2021 over different basins of India. The green/ yellow shade represents a significant positive/ negative trend at a 95% confidence level. (For interpretation of the references to colour in this figure legend, the reader is referred to the web version of this article.)

generated per unit rainfall. Similarly, a positive RE trend is detected in Brahmaputra while precipitation and runoff don't show statistically significant trend. In the pre-monsoon season, a significant RE trend has been observed in WFKS, Krishna, and EFPK despite there is no trend in rainfall and runoff (See supplementary Fig. S5). This increasing trend in RE over different basins shows the accelerated response of the water cycle owing to climate change (Wang et al., 2023).

## 4. Conclusions and future work

Runoff efficiency (RE) is an ideal diagnostic tool to study the hydrological performance of a basin. First, we explored the spatio-temporal variability of RE over different basins of South Asia and studied the role of climatology and basin physiography. Then, we studied the role of ENSO on the temporal RE variability. Finally, the long-term variability of RE has been examined using trend analysis. The major findings from this study have been highlighted below.

- The spatial variability of RE is primarily controlled by the relative effect of climate and soil type. The Central Indian basins such as Narmada, Godavari, Tapi, Mahanadi, and Brahmani are observed to be hydrological active basins pertaining to the high mean annual precipitation and low permeable soil. Ganga, Brahmaputra, and Subarnarekha exhibit low RE despite high mean rainfall due to moderate permeable soil type and higher baseflow contribution. West flowing basins have relatively less RE despite receiving very high mean monsoon rainfall due to the forest land cover and moderately permeable soil type.
- Temporal variability of Monthly RE is mainly controlled by the relative effect of monthly precipitation magnitude, antecedent soil moisture condition (AMC), and seasonality. The three factors exhibit certain levels of interdependency and also the effect of AMC is relatively higher than precipitation magnitude.
- El Niño-Southern Oscillation (ENSO) is an external factor that modulates the temporal variability of RE. During the Monsoon, ENSO significantly affects the rainfall of Central eastern, Central, and Peninsular basins with La Niña phase enhancing the rainfall. The ENSO impact on rainfall is amplified on the runoff resulting in significant modulation on RE. The ENSO impact is reversed in the winter season where the La Niña depreciates the rainfall in Northern India, however, the influence is not reflected in the RE. Winter ENSO affects the Southern basins such as Cauvery and East Flowing Pennar-Kanyakumari (EFPK) causing a higher rainfall in La Niña phases and RE also shows a significant impact.
- Long-term trends are found in RE over different regions which vary with season. West Flowing Kachh-Sabarmati basins show a significant positive trend in monsoon, pre-monsoon, and winter. In many basins, the rainfall and runoff don't show a trend while the RE has shown a positive trend. This increasing trend in RE over different basins without any trend in rainfall shows the accelerated response of the water cycle owing to climate change.

Overall, this comprehensive study of the behavior of RE over the South Asian River basins, concludes that RE is influenced by both climatology and basin physiography. Monitoring changing RE has implications for water availability, flash floods, erosion, etc. Further, improving understanding of RE can enhance runoff prediction skills. The future scope of the study would be investigating the behavior of RE variability during hydrological extremes such as floods and droughts.

## CRediT authorship contribution statement

**V.V. Sidhan:** Conceptualization, Methodology, Formal analysis, Writing – original draft. **Manabendra Saharia:** Writing – review & editing, Supervision, Resources, Project administration, Funding acquisition, Data curation, Conceptualization.

## Declaration of competing interest

The authors declare that they have no known competing financial interests or personal relationships that could have appeared to influence the work reported in this paper.

## Acknowledgements

The study was carried out in the IIT Delhi HydroSense lab (https://hydrosense.iitd.ac.in/), and the authors thank the IIT Delhi High Performance Computing facility for supplying the computational and storage resources. Dr. Manabendra Saharia expresses gratitude for grants that provided funding for this work such as ISRO Space Technology Cell (STC0374/RP04139); MoES Monsoon Mission III (RP04574); and DST IC-IMPACTS (RP04558). The authors would also like to thank Mr. Priyam Deka.

*Compliance with ethical standards*

The authors declare that none of the work reported in this study could have been influenced by any known competing financial interests or personal relationships.

## Appendix A. Supplementary data

Supplementary data to this article can be found online at https://doi.org/10.1016/j.jhydrol.2025.132680.

## Data availability

The following sources provide the datasets used in this study:

IMD precipitation: https://www.imdpune.gov.in/Clim_Pred_LRF_New/.

Streamflow: Central Water Commission, India, and India WRIS, https://indiawris.gov.in/wris/.

MERRA-2: GMAO, NASA Goddard Space Flight Centre, https://disc.gsfc.nasa.gov/datasets?project=MERRA-2.

MODIS Evapotranspiration: GSFC, NASA, https://modis.gsfc.nasa.gov/data/dataprod/mod16.php.

The data that support the findings are available on request from the corresponding author.

## References

Abdulkareem, J.H., Pradhan, B., Sulaiman, W.N.A., Jamil, N.R., 2018. Quantification of Runoff as Influenced by Morphometric Characteristics in a Rural Complex Catchment. Earth Syst. Environ. 2 (1), 145–162. https://doi.org/10.1007/s41748-018-0043-0.

Agnihotri, I., Punia, D. M. P., & Sharma, D. J. R. (2017). Trend Analysis Of Precipitation Data And Its Spatio-Temporal Assessment in West Flowing River Basin Of Kutch, Saurashtra, And Marwar (WFR-KSM) Basin, India.

Agnihotri, I., Punia, M.P., Sharma, J.R., 2018. Assessment of Spatial Variations in Temperature and Precipitation Extremes in West-Flowing River Basin of Kutch, Saurashtra and Marwar, India. Curr. Sci. 114 (02), 322. https://doi.org/10.18520/cs/v114/i02/322-328.

Ahmad, N., 1996. Occurrence and Distribution of Vertisols. in Developments in Soil Science 24, 1–41.

Akhil, R., Prasad, T., Vineethkumar, V., 2022. Analyzing the significance of morphometric parameters in runoff efficiency: A case study in Valakkayi Tode tropical watershed, Valapattanam River, Kerala, India. J. Sedimentary Environ. 1–12.

Allan, R.P., Barlow, M., Byrne, M.P., Cherchi, A., Douville, H., Fowler, H.J., Gan, T.Y., Pendergrass, A.G., Rosenfeld, D., Swann, A.L.S., Wilcox, L.J., Zolina, O., 2020. Advances in understanding large-scale responses of the water cycle to climate change. Ann. N. Y. Acad. Sci. 1472 (1), 49–75. https://doi.org/10.1111/nyas.14337.

Astuti, I.S., Sahoo, K., Milewski, A., Mishra, D.R., 2019. Impact of Land Use Land Cover (LULC) Change on Surface Runoff in an Increasingly Urbanized Tropical Watershed. Water Resour. Manag. 33 (12), 4087–4103. https://doi.org/10.1007/s11269-019-02320-w.

Burn, D.H., Cunderlik, J.M., Pietroniro, A., 2004. Hydrological trends and variability in the Liard River basin / Tendances hydrologiques et variabilité dans le basin de la

rivière Liard. Hydrol. Sci. J. 49 (1), 53–67. https://doi.org/10.1623/hysj.49.1.53.53994.
Chandole, V., Joshi, G.S., Rana, S.C., 2019. Spatio -temporal trend detection of hydro -meteorological parameters for climate change assessment in Lower Tapi river basin of Gujarat state, India. J. Atmos. Sol. Terr. Phys. 195, 105130. https://doi.org/10.1016/j.jastp.2019.105130.
Dimri, A.P., 2013. Relationship between ENSO phases with Northwest India winter precipitation. Int. J. Climatol. 33 (8), 1917–1923. https://doi.org/10.1002/joc.3559.
Durack, P.J., Wijffels, S.E., Matear, R.J., 2012. Ocean Salinities Reveal Strong Global Water Cycle Intensification During 1950 to 2000. Science 336 (6080), 455–458. https://doi.org/10.1126/science.1212222.
Frans, C., Istanbulluoglu, E., Mishra, V., Munoz-Arriola, F., Lettenmaier, D.P., 2013. Are climatic or land cover changes the dominant cause of runoff trends in the Upper Mississippi River Basin? Geophys. Res. Lett. 40 (6), 1104–1110. https://doi.org/10.1002/grl.50262.
Gadgil, S., Rajeevan, M., Francis, P.A., 2007. Monsoon variability: Links to major oscillations over the equatorial Pacific and Indian oceans. Curr. Sci. 93 (2).
Graham, N., 1994. Decadal-scale climate variability in the tropical and North Pacific during the 1970s and 1980s: Observations and model results. Clim. Dyn. 10, 135–162.
Guhathakurta, P., Rajeevan, M., 2008. Trends in the rainfall pattern over India. Int. J. Climatol. 28 (11), 1453–1469. https://doi.org/10.1002/joc.1640.
Gunnell, Y., 1997. Relief and climate in South Asia: The influence of the western ghats on the current climate pattern of peninsular India. Int. J. Climatol. 17 (11), 1169–1182. https://doi.org/10.1002/(SICI)1097-0088(199709)17:11<1169::AID-JOC189>3.0.CO;2-W.
Hernandez, D., Mendoza, P.A., Boisier, J.P., Ricchetti, F., 2022. Hydrologic Sensitivities and ENSO Variability Across Hydrological Regimes in Central Chile (28°–41°S). Water Resour. Res. 58 (9), e2021WR031860. https://doi.org/10.1029/2021WR031860.
Hrudya, P.H., Varikoden, H., Vishnu, R., 2021. A review on the Indian summer monsoon rainfall, variability and its association with ENSO and IOD. Meteorol. Atmos. Phys. 133 (1), 1–14. https://doi.org/10.1007/s00703-020-00734-5.
Huntington, T.G., 2006. Evidence for intensification of the global water cycle: Review and synthesis. J. Hydrol. 319 (1–4), 83–95. https://doi.org/10.1016/j.jhydrol.2005.07.003.
Hussain, A., Cao, J., Ali, S., Ullah, W., Muhammad, S., Hussain, I., Rezaei, A., Hamal, K., Akhtar, M., Abbas, H., Wu, X., Zhou, J., 2022. Variability in runoff and responses to land and oceanic parameters in the source region of the Indus River. Ecol. Ind. 140, 109014. https://doi.org/10.1016/j.ecolind.2022.109014.
Jain, S.K., Kumar, V., Saharia, M., 2013. Analysis of rainfall and temperature trends in northeast India. Int. J. Climatol. 33 (4), 968–978.
Joshi, N., Gupta, D., Suryavanshi, S., Adamowski, J., Madramootoo, C.A., 2016. Analysis of trends and dominant periodicities in drought variables in India: A wavelet transform based approach. Atmos. Res. 182, 200–220. https://doi.org/10.1016/j.atmosres.2016.07.030.
Kaur, S., Diwakar, S.K., Das, A.K., 2017. Long term rainfall trend over meteorological sub divisions and districts of India. Mausam 68 (3), 439–450. https://doi.org/10.54302/mausam.v68i3.676.
Kirnbauer, R., Blöschl, G., Haas, P., Müller, G., Merz, B., 2005. Identifying Space-time Patterns of Runoff Generation: A Case Study from the Löhnersbach Catchment, Austrian Alps. In: Huber, U.M., Bugmann, H.K.M., Reasoner, M.A. (Eds.), Global Change and Mountain Regions, Vol. 23. Springer, Netherlands, pp. 309–320. https://doi.org/10.1007/1-4020-3508-X_31.
Krishnamurthy, L., Krishnamurthy, V., 2016. Decadal and interannual variability of the Indian Ocean SST. Clim. Dyn. 46 (1–2), 57–70. https://doi.org/10.1007/s00382-015-2568-3.
Krishnamurthy, V., Goswami, B.N., 2000. Indian Monsoon–ENSO Relationship on Interdecadal Timescale. J. Clim. 13 (3), 579–595. https://doi.org/10.1175/1520-0442(2000)013<0579:IMEROI>2.0.CO;2.
Krishnan, R., Kumar, V., Sugi, M., Yoshimura, J., 2009. Internal Feedbacks from Monsoon–Midlatitude Interactions during Droughts in the Indian Summer Monsoon. J. Atmos. Sci. 66 (3), 553–578. https://doi.org/10.1175/2008JAS2723.1.
Krishnan, R., Sanjay, J., Gnanaseelan, C., Mujumdar, M., Kulkarni, A., & Chakraborty, S. (Eds.). (2020). Assessment of Climate Change over the Indian Region: A Report of the Ministry of Earth Sciences (MoES), Government of India. Springer Singapore. https://doi.org/10.1007/978-981-15-4327-2.
Kumar, S., Peterslidard, C., Tian, Y., Houser, P., Geiger, J., Olden, S., Lighty, L., Eastman, J., Doty, B., Dirmeyer, P., 2006. Land information system: An interoperable framework for high resolution land surface modeling. Environ. Model. Softw. 21 (10), 1402–1415. https://doi.org/10.1016/j.envsoft.2005.07.004.
Kumar, S., Ranta, M., & Praveen, T. (2010). Analysis of the run off for watershed using SCS-CN method and geographic information systems.
Lee, H., Calvin, K., Dasgupta, D., Krinner, G., Mukherji, A., Thorne, P., Trisos, C., Romero, J., Aldunce, P., & Barret, K. (2023). IPCC, 2023: Climate Change 2023: Synthesis Report, Summary for Policymakers. Contribution of Working Groups I, II and III to the Sixth Assessment Report of the Intergovernmental Panel on Climate Change [Core Writing Team, H. Lee and J. Romero (eds.)]. IPCC, Geneva, Switzerland.
Magotra, B., Prakash, V., Saharia, M., Getirana, A., Kumar, S., Pradhan, R., Dhanya, C.T., Rajagopalan, B., Singh, R.P., Pandey, A., Mohapatra, M., 2024. Towards an Indian land data assimilation system (ILDAS): A coupled hydrologic-hydraulic system for water balance assessments. J. Hydrol. 629, 130604. https://doi.org/10.1016/j.jhydrol.2023.130604.
Mangan, P., Haq, M.A., Baral, P., 2019. Morphometric analysis of watershed using remote sensing and GIS—a case study of Nanganji River Basin in Tamil Nadu. India. Arabian Journal of Geosciences 12 (6), 202. https://doi.org/10.1007/s12517-019-4382-4.
Mann, H.B., 1945. Nonparametric Tests Against Trend. Econometrica 13 (3), 245. https://doi.org/10.2307/1907187.
McCabe, G.J., Wolock, D.M., 2016. Variability and Trends in Runoff Efficiency in the Conterminous United States. JAWRA Journal of the American Water Resources Association 52 (5), 1046–1055. https://doi.org/10.1111/1752-1688.12431.
Merz, R., Blöschl, G., 2009. A regional analysis of event runoff coefficients with respect to climate and catchment characteristics in Austria. Water Resour. Res. 45 (1), 2008WR007163. https://doi.org/10.1029/2008WR007163.
Merz, R., Blöschl, G., Parajka, J., 2006. Spatio-temporal variability of event runoff coefficients. J. Hydrol. 331 (3–4), 591–604. https://doi.org/10.1016/j.jhydrol.2006.06.008.
Meshram, S.G., Singh, V.P., Meshram, C., 2017. Long-term trend and variability of precipitation in Chhattisgarh State, India. Theoretical and Applied Climatology 129 (3–4), 729–744. https://doi.org/10.1007/s00704-016-1804-z.
Niu, G., Yang, Z., Mitchell, K.E., Chen, F., Ek, M.B., Barlage, M., Kumar, A., Manning, K., Niyogi, D., Rosero, E., 2011. The community Noah land surface model with multiparameterization options (Noah-MP): 1. Model description and evaluation with local-scale measurements. J. Geophys. Res. Atmos. 116 (D12).
Norbiato, D., Borga, M., Merz, R., Blöschl, G., Carton, A., 2009. Controls on event runoff coefficients in the eastern Italian Alps. J. Hydrol. 375 (3–4), 312–325. https://doi.org/10.1016/j.jhydrol.2009.06.044.
Nowak, K., Hoerling, M., Rajagopalan, B., Zagona, E., 2012. Colorado River Basin Hydroclimatic Variability. J. Clim. 25 (12), 4389–4403. https://doi.org/10.1175/JCLI-D-11-00406.1.
Pai, D., Sridhar, L., Badwaik, M., Rajeevan, M., 2015. Analysis of the daily rainfall events over India using a new long period (1901–2010) high resolution (0.25× 0.25) gridded rainfall data set. Clim. Dyn. 45, 755–776.
Rajeevan, M., Unnikrishnan, C.K., Bhate, J., Niranjan Kumar, K., Sreekala, P.P., 2012. Northeast monsoon over India: Variability and prediction. Meteorol. Appl. 19 (2), 226–236. https://doi.org/10.1002/met.1322.
Ross, C.W., Prihodko, L., Anchang, J., Kumar, S., Ji, W., Hanan, N.P., 2018. HYSOGs250m, global gridded hydrologic soil groups for curve-number-based runoff modeling. Sci. Data 5 (1), 180091. https://doi.org/10.1038/sdata.2018.91.
Sivakumar, M.V.K., Stefanski, R., 2010. Climate Change in South Asia. In: Lal, R., Sivakumar, M.V.K., Faiz, S.M.A., Mustafizur Rahman, A.H.M., Islam, K.R. (Eds.), Climate Change and Food Security in South Asia. Springer, Netherlands, pp. 13–30. https://doi.org/10.1007/978-90-481-9516-9_2.
Sivapalan, M., 2005. Pattern, Process and Function: Elements of a Unified Theory of Hydrology at the Catchment Scale. In: Anderson, M.G., McDonnell, J.J. (Eds.), Encyclopedia of Hydrological Sciences, (1st ed.). Wiley. https://doi.org/10.1002/0470848944.hsa012.
Soden, B.J., 2000. The Sensitivity of the Tropical Hydrological Cycle to ENSO. J. Clim. 13 (3), 538–549. https://doi.org/10.1175/1520-0442(2000)013<0538:TSOTTH>2.0.CO;2.
Swanson, K.L., Tsonis, A.A., 2009. Has the climate recently shifted? Geophys. Res. Lett. 36 (6), 2008GL037022. https://doi.org/10.1029/2008GL037022.
Trenberth, K.E., 1997. The Definition of El Niño. Bull. Am. Meteorol. Soc. 78 (12), 2771–2777. https://doi.org/10.1175/1520-0477(1997)078<2771:TDOENO>2.0.CO;2.
Trenberth, K.E., Stepaniak, D.P., 2001. Indices of El Niño Evolution. J. Clim. 14 (8), 1697–1701. https://doi.org/10.1175/1520-0442(2001)014<1697:LIOENO>2.0.CO;2.
Wang, Y., Ye, A., Zhang, Y., Yang, F., 2023. The quantitative attribution of climate change to runoff increase over the Qinghai-Tibetan Plateau. Sci. Total Environ. 897, 165326. https://doi.org/10.1016/j.scitotenv.2023.165326.
Woodhouse, C.A., Pederson, G.T., 2018. Investigating Runoff Efficiency in Upper Colorado River Streamflow Over Past Centuries. Water Resour. Res. 54 (1), 286–300. https://doi.org/10.1002/2017WR021663.
Yadav, S.M., Bhagat, S.R., Yadav, V.G., 2021. Temporal analysis of precipitation in Saurashtra, Kutch, and Diu sub-division of Western Indian region. Theor. Appl. Climatol. 144 (1–2), 521–533. https://doi.org/10.1007/s00704-021-03564-6.
Zhang, X., Harvey, K.D., Hogg, W.D., Yuzyk, T.R., 2001. Trends in Canadian streamflow. Water Resour. Res. 37 (4), 987–998. https://doi.org/10.1029/2000WR900357.